Age of Information in Slotted ALOHA With Energy Harvesting

Khac-Hoang Ngo*, Giuseppe Durisi*, Alexandre Graell i Amat*, Andrea Munari†, and Francisco Lázaro†

*Department of Electrical Engineering, Chalmers University of Technology, 41296 Gothenburg, Sweden
†Institute for Communications and Navigation, German Aerospace Center (DLR), 82234 Weßling, Germany

Abstract—We examine the age of information (AoI) of a status update system that incorporates energy harvesting and uses the slotted ALOHA protocol. We derive analytically the average AoI and the probability that the AoI exceeds a given threshold. Via numerical results, we investigate two strategies to minimize the age of information (AoI): transmitting a new update whenever possible to exploit every chance to reduce the AoI, and transmitting only when sufficient energy is available to increase the chance of successful delivery. The two strategies are beneficial for low and high update generation rates, respectively. However, an optimized approach that balances the two strategies outperforms them significantly in terms of both AoI and throughput.

I. INTRODUCTION

In delay-sensitive Internet of Things (IoT) applications, devices need to deliver timely status updates to a central gateway. To measure the freshness of status updates, the AoI metric has been introduced (see, e.g., [1] and references therein). It captures the time elapsed since the generation of the last update available at the gateway. Recent studies have characterized the AoI for random-access medium sharing protocols, such as slotted ALOHA [2], [3] and its modern variations [4]–[6].

IoT devices are designed for low-power, long-term operation and can be placed in remote or hard-to-reach locations, hindering battery replacement. A solution to these challenges is energy harvesting, which allows IoT devices to capture and convert energy from the environment into electrical energy [7]. The AoI of energy-harvesting devices has been analyzed mainly for the single-source scenario [8], [9]. Existing analyses of ALOHA-based random-access protocols with energy harvesting focused on stability [10] and throughput [11], [12]. Compared to the setting in [2]–[6], energy harvesting introduces new factors that significantly affect information freshness, such as the level of available energy at the devices at the time of update generation, and the need for the devices to spend time harvesting energy. However, the impact of energy harvesting on the AoI in random-access protocols remains widely unexplored.

This paper characterizes the behavior of the AoI in a slotted-ALOHA status update system with energy harvesting. We model energy hervesting as independent Bernoulli processes. We assume that each device receives readings from a sensor, and thus cannot generate fresh updates at will. Upon receiving a new reading, the device transmits the update with a probability adapted to its battery level. A transmitted update is correctly decoded with a probability that depends on the transmit power and the level of interference from other devices. By means of a Markovian analysis, we derive the average AoI analytically for a given transmission probability. We further provide an approximate analysis that results in easy-to-compute and accurate approximations of both the average AoI and the age-violation probability (AVP), which is the probability that the AoI exceeds a given threshold.

In our numerical experiments, we assume that each slot comprises multiple uses of an additive white Gaussian noise (AWGN) channel. We consider both decoding without capture, where the receiver performs decoding only in slots containing a single update, and decoding with capture, where the receiver attempts decoding in each slot using successive interference cancellation (SIC) to recover colliding packets. We investigate the importance of optimally adapting the transmission probability to the available energy. On the one hand, transmitting a new update whenever possible (a.k.a. best-effort uniform policy [8], [9]) exploits every opportunity to reduce the AoI, but increases channel traffic and the risk of losing the update if the transmit power is insufficient. On the other hand, transmitting only with high power increases the chance of successful delivery, but requires devices to ignore some updates while harvesting enough energy. Taking these two strategies as baselines, we compare them with the optimized transmission probability that minimizes the average AoI, minimizes the AVP, or maximizes the throughput. Numerical results show that significant gains in all three metrics are achieved with the optimized strategy for both decoding with and without capture. Transmitting an update whenever possible is close to optimal for low update generation rates but performs poorly for high update generation rates. As the update generation rate increases, transmitting only when the battery is full has a decreasing gap to the optimal performance without capture. However, this strategy does not benefit from decoding with capture. Furthermore, the strategy optimized for throughput entails a loss in average AoI and AVP, especially for high update generation rates. Finally, decoding with capture outperforms significantly decoding without capture for the optimized strategy.

Notation: We let $[m:n] = \{m, m+1, \ldots, n\}$, $[n] = [1:n]$, and $x^+ = \max\{0, x\}$. We denote by $\mathbf{I}_m$ the $m \times m$ identity matrix, $\mathbf{0}_m$ the $m \times 1$ all-zero vector, $\mathbf{1}_m$ the $m \times 1$ all-one vector, $[\boldsymbol{x}]_1$ the first entry of $\boldsymbol{x}$, and $\mathbb{1}\{\cdot\}$ the indicator function.

Reproducible Research: The Matlab code used to generate our numerical results is available at: github.com/khachoang1412/AoI_slottedALOHA_energyHarvesting.

Fig. 1: Example of the AoI process.
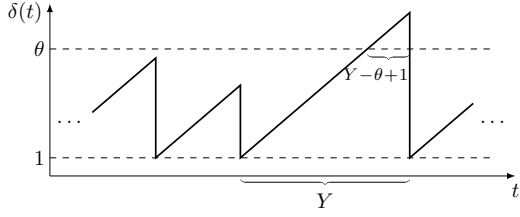

Fig. 2: Markov chain M_1 describing the battery level of a device.

II. SYSTEM MODEL

We consider a system with U devices attempting to deliver time-stamped status updates (also called packets) to a gateway through a wireless channel. We assume that the updates are generated independently across devices. Time is slotted and the devices are slot-synchronous. Each update transmission spans a slot. A device receives a new sensor reading at the beginning of each slot with probability (w.p.) α.

1) Energy Harvesting: Each device is equipped with a rechargeable battery with capacity E energy units. The devices harvest energy from the environment to recharge their batteries. In each slot, one energy unit is harvested by a device w.p. η, independently of the other slots and other devices. If the battery is full, the device pauses harvesting. We denote by ν_b (computed in Section III) the steady-state probability that the battery level of an arbitrary device is $b \in [0 : E]$.

2) Medium Access Protocol: The devices access the medium following the slotted ALOHA protocol. Specifically, if a device has a new update in a slot, it transmits the update w.p. π_b if its battery level is b. Obviously, $\pi_0 = 0$, while $\boldsymbol{\pi} = (\pi_1, \ldots, \pi_E)$ is a design parameter. We assume that the devices always spend all available energy to transmit a packet.[1] Furthermore, as in [10], [11], we assume that the devices can either transmit or harvest energy in a slot. No feedback is provided by the receiver.

Consider a device that transmits with b energy units in a slot and assume that the *battery profile* of the remaining devices is $\boldsymbol{L} = (L_0, \ldots, L_E)$, i.e., L_i out of the remaining $U - 1$ devices have battery level $i \in [0 : E]$. We denote by $w_{b,\boldsymbol{L}}$ the probability that an update transmitted with b energy units is correctly decoded when the battery profile of the other devices is $\boldsymbol{L}$. The dependency of $w_{b,\boldsymbol{L}}$ on b and $\boldsymbol{L}$ captures the impact of the transmit power and of the interference from the other devices. All analytical results in the paper hold for general $w_{b,\boldsymbol{L}}$, while in Section VI, we shall instantiate $w_{b,\boldsymbol{L}}$ by considering an AWGN channel. At steady state, the average successful delivery probability of a device that transmits with b energy units is

$$\bar{w}_b = \mathbb{E}_{\boldsymbol{L}}[w_{b,\boldsymbol{L}}] \qquad (1)$$

where $\boldsymbol{L}$ follows the multinomial distribution with number of trials $U - 1$, number of events $E + 1$, and event probabilities $\{\nu_i\}_{i=0}^{E}$. The average throughput, i.e., the average number of packets decoded per slot, is given by $S = \alpha U \sum_{b=0}^{E} \nu_b \pi_b \bar{w}_b$.

3) Age of Information: We define the AoI of a generic device at slot t as $\delta(t) = t - \tau(t)$, where $\tau(t)$ denotes the timestamp

[1]We shall address the general case where the devices transmit using only part of the available energy in an extension of this paper.
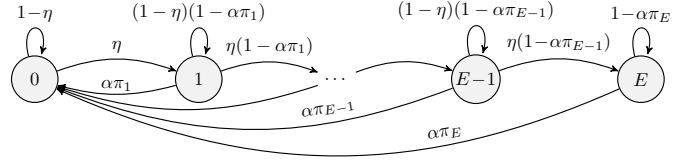
of the last received update from this device as of slot t. The corresponding stochastic process is denoted as $\Delta(t)$. The AoI grows linearly with time and is reset to 1 when a new update is successfully decoded. It has a saw-tooth shape as illustrated in Fig. 1. We are interested in the average AoI $\bar{\Delta} = \mathbb{E}[\Delta(t)]$ and the AVP $\zeta(\theta) = \mathbb{P}[\Delta(t) > \theta]$.

III. BATTERY EVOLUTION

1) Battery Level of a Generic Device: The evolution of the battery level of a generic device is captured by the Markov chain M_1 shown in Fig. 2. Each state represents a battery level. The transition probabilities between the states can be readily computed. Specifically, a device in state 0 cannot transmit, thus it either remains in this state if it does not harvest energy (w.p. $1 - \eta$) or jumps to state 1 if an energy unit arrives (w.p. η). A device in state $i \in [E]$ moves to state 0 if it generates and transmits a new update (w.p. $\alpha \pi_i$). Otherwise, if $i < E$, the device either remains in state i if no energy is harvested (w.p. $(1 - \eta)(1 - \alpha \pi_i)$) or jumps to state $i + 1$ if an energy unit is harvested (w.p. $\eta(1 - \alpha \pi_i)$). If the battery is full, i.e., $i = E$, the device remains in state E if it does not transmit (w.p. $1 - \alpha \pi_i$). From these transition probabilities, we compute the steady-state distribution $\{\nu_b\}_{b=0}^{E}$ by solving the balance equations.

2) Battery Profile of $U - 1$ Devices: The battery profile $\boldsymbol{L}$ of the other $U - 1$ devices can take values in $\mathcal{L} = \left\{ (\ell_0, \ell_1, \ldots, \ell_E) : \sum_{i=0}^{E} \ell_i = U - 1, \ell_i \in [0 : U - 1], i \in [0 : E] \right\}$. We now describe the evolution of $\boldsymbol{L}$ within a slot. Let $\boldsymbol{\ell}' = (\ell_0', \ell_1', \ldots, \ell_E')$ and $\boldsymbol{\ell} = (\ell_0, \ell_1, \ldots, \ell_E)$ denote the states at the beginning and the end of a slot, respectively. Let also $u_{j,k}$ be the number of devices whose battery goes from level j to level k. We have that

$$u_{j,k} \in [0 : \min\{\ell_j', \ell_k\}], \quad j, k \in [0 : E], \qquad (2)$$
$$\ell_0' = u_{0,0} + u_{0,1}, \qquad (3)$$
$$\ell_i' = u_{i,i} + u_{i,0} + u_{i,i+1}, \quad i \in [1 : E - 1], \qquad (4)$$
$$\ell_E' = u_{E,E} + u_{E,0}, \qquad (5)$$
$$\ell_0 = u_{0,0} + \sum_{i=1}^{E} u_{i,0}, \qquad (6)$$
$$\ell_i = u_{i,i} + u_{i-1,i}, \quad i \in [E]. \qquad (7)$$

hence, the transition probability $\mathbb{P}[\boldsymbol{\ell}' \to \boldsymbol{\ell}]$ is

$$\mathbb{P}[\boldsymbol{\ell}' \to \boldsymbol{\ell}] = \sum_{\{u_{j,k}\} : (2)-(7)} \left(\prod_{j,k \in [0:E]} p_{j,k}^{u_{j,k}} \right)$$
$$\cdot \binom{\ell_0'}{u_{0,0}} \binom{\ell_E'}{u_{E,0}} \prod_{j=1}^{E-1} \binom{\ell_j'}{u_{j,0}} \binom{\ell_j' - u_{j,0}}{u_{j,j}}, \qquad (8)$$

where $p_{j,k}$ is the transition probability from state j to state k of the Markov chain M_1 in Fig. 2.

IV. AoI Analysis

We now derive the average AoI of a generic device.

1) Preliminaries: We denote by $B^{(s)}$ the battery level of the device of interest at the end of slot s. We let $X^{(s)} = \text{S}$ (standing for "success") if the device successfully delivers an update in the slot, and $X^{(s)} = \text{F}$ (standing for "fail") otherwise. Furthermore, we denote the battery profile of the remaining $U-1$ devices at the end of slot s by $\boldsymbol{L}^{(s)} = (L_0^{(s)}, \ldots, L_E^{(s)})$. Consider an ancillary Markov chain $Z^{(s)} = (X^{(s)}, B^{(s)}, \boldsymbol{L}^{(s)})$. We next derive the transition probability from state $(x', b', \boldsymbol{\ell}')$ to state $(x, b, \boldsymbol{\ell})$. If $X^{(s-1)} = \text{S}$, the device of interest depletes its battery and thus cannot transmit an update in slot s. Therefore,

$$\mathbb{P}\big[(\text{S},0,\boldsymbol{\ell}') \to (x,b,\boldsymbol{\ell})\big] = \mathbb{1}\{x = \text{S}\}$$
$$\cdot ((1-\eta)\mathbb{1}\{b=0\} + \eta\mathbb{1}\{b=1\})\mathbb{P}\big[\boldsymbol{\ell}' \to \boldsymbol{\ell}\big], \qquad (9)$$

where $\mathbb{P}\big[\boldsymbol{\ell}' \to \boldsymbol{\ell}\big]$ is given in (8). If $X^{(s-1)} = \text{F}$, we separate the cases $X^{(s)} = \text{S}$ and $X^{(s)} = \text{F}$. First, $X^{(s)} = \text{S}$ if in slot s the device generates and transmits a new update (w.p. $\alpha\pi_{b'}$), and the update is successfully decoded (w.p. $w_{b',\boldsymbol{\ell}'}$). In this case, the device depletes its battery after slot s. Therefore,

$$\mathbb{P}\big[(\text{F},b',\boldsymbol{\ell}') \to (\text{S},b,\boldsymbol{\ell})\big] = \alpha\pi_{b'} w_{b',\boldsymbol{\ell}'}\mathbb{1}\{b=0\}\mathbb{P}\big[\boldsymbol{\ell}' \to \boldsymbol{\ell}\big]. \quad (10)$$

Second, $X^{(s)} = \text{F}$ if in slot s the device either does not transmit or transmits but fails to deliver the packet. It follows that

$$\mathbb{P}\big[(\text{S},b',\boldsymbol{\ell}') \to (\text{F},b,\boldsymbol{\ell})\big]$$
$$= \big[(1 - \alpha\pi_{b'}\mathbb{1}\{b' > 0\})\big((1-\eta)\mathbb{1}\{b' = b < E\}$$
$$+ \eta\mathbb{1}\{b = b' + 1\} + \mathbb{1}\{b = b' = E\}\big)$$
$$+ \alpha\pi_{b'}(1 - w_{b',\boldsymbol{\ell}'})\mathbb{1}\{b=0\}\big]\mathbb{P}\big[\boldsymbol{\ell}' \to \boldsymbol{\ell}\big]. \quad (11)$$

2) Average AoI: As shown in Fig. 1, we denote by Y the *inter-refresh* time, i.e., the number of slots that elapse between two successive status updates for the device of interest. Right after a refresh, the current AoI is set to 1. By proceeding as in [1, Sec. II-A] or [3, Sec. III], we observe that the average AoI can be expressed in terms of the moments of Y as

$$\bar{\Delta} = 1 + \frac{\mathbb{E}\big[Y^2\big]}{2\mathbb{E}[Y]}. \qquad (12)$$

We next derive the moments of Y. Without loss of generality, we assign index 1 to the first slot contributing to the current inter-refresh time. We expand $\mathbb{E}[Y]$ as

$$\mathbb{E}[Y] = \sum_{x \in \{\text{F,S}\}} \sum_{b \in [0:E]} \sum_{\boldsymbol{\ell} \in \mathcal{L}} \mathbb{E}\big[Y|Z^{(1)} = (x,b,\boldsymbol{\ell})\big]$$
$$\cdot \mathbb{P}\big[Z^{(1)} = (x,b,\boldsymbol{\ell})\big]. \qquad (13)$$

To compute $\mathbb{P}\big[Z^{(1)} = (x,b,\boldsymbol{\ell})\big]$, we note that the state at the end of a slot with AoI refresh is of the form $(\text{S},0,\boldsymbol{\ell})$, and the state at the end of slot 1 can only be $(\text{F},0,\boldsymbol{\ell})$ or $(\text{F},1,\boldsymbol{\ell})$. Therefore,

$$\mathbb{P}\big[Z^{(1)} = (x,b,\boldsymbol{\ell})\big] = \mathbb{1}\{x = \text{F}, b \in \{0,1\}\}$$

$$\cdot \frac{\sum_{\boldsymbol{\ell}' \in \mathcal{L}} \mathbb{P}\big[(\text{S},0,\boldsymbol{\ell}') \to (\text{F},b,\boldsymbol{\ell})\big]}{\sum_{b \in \{0,1\}, \boldsymbol{\ell} \in \mathcal{L}} \sum_{\boldsymbol{\ell}' \in \mathcal{L}} \mathbb{P}\big[(\text{S},0,\boldsymbol{\ell}') \to (\text{F},b,\boldsymbol{\ell})\big]}. \qquad (14)$$

The conditional expectation $\mathbb{E}\big[Y|Z^{(1)} = (x,b,\boldsymbol{\ell})\big]$ can be derived via a first-step analysis [13, Sec. III-4]. If the packet from the device of interest is decoded in slot 1, i.e., $X^{(s)} = 1$, the inter-refresh time is 1. It follows that

$$\mathbb{E}\big[Y|Z^{(1)} = (\text{S},b,\boldsymbol{\ell})\big] = 1, \quad b \in [0:E], \boldsymbol{\ell} \in \mathcal{L}. \qquad (15)$$

If $Z^{(1)} = (\text{F},b,\boldsymbol{\ell})$, the inter-refresh time can be computed as the sum of the number of slots until a transmitted packet is successfully decoded. This can be conveniently computed by conditioning on the outcome of the first transition. Specifically, we define $r(b,\boldsymbol{\ell}) = \sum_{b'' \in [0:E], \boldsymbol{\ell}'' \in \mathcal{L}} \mathbb{P}\big[(\text{F},b,\boldsymbol{\ell}) \to (\text{S},b'',\boldsymbol{\ell}'')\big]$, $q((b,\boldsymbol{\ell}) \to (b'',\boldsymbol{\ell}'')) = \mathbb{P}\big[(\text{F},b,\boldsymbol{\ell}) \to (\text{F},b'',\boldsymbol{\ell}'')\big]$, and proceed as

$$\mathbb{E}\big[Y|Z^{(1)} = (\text{F},b,\boldsymbol{\ell})\big] =$$
$$1 + \sum_{z \in \{\text{F,S}\} \times [0:E] \times \mathcal{L}} \mathbb{E}\big[Y|Z^{(1)} = z\big]\mathbb{P}[(\text{F},b,\boldsymbol{\ell}) \to z] \quad (16)$$
$$= 1 + r(b,\boldsymbol{\ell})$$
$$+ \sum_{b'' \in [0:E], \boldsymbol{\ell}'' \in \mathcal{L}} \mathbb{E}\big[Y|Z^{(1)} = (\text{F},b'',\boldsymbol{\ell}'')\big]$$
$$\cdot q((b,\boldsymbol{\ell}) \to (b'',\boldsymbol{\ell}'')). \qquad (17)$$

In (16), the Markov property ensures that the average duration, once the transition to state z has occurred, is equal to the one that we would have by starting from such state. Let $\boldsymbol{e}$ and $\boldsymbol{r}$ be vectors that contain $\mathbb{E}\big[Y|Z^{(1)} = (\text{F},b,\boldsymbol{\ell})\big]$ and $r(b,\boldsymbol{\ell})$, respectively, for all values of $(b,\boldsymbol{\ell})$. Let $\mathbf{Q}$ be a matrix that contains $q((b,\boldsymbol{\ell}) \to (b'',\boldsymbol{\ell}''))$ for all $(b,\boldsymbol{\ell})$ and $(b'',\boldsymbol{\ell}'')$. The full-rank system of equations obtained from (17) can be expressed compactly as $(\mathbf{I}-\mathbf{Q})\boldsymbol{e} = \boldsymbol{1}+\boldsymbol{r}$. Therefore, $\boldsymbol{e} = (\mathbf{I}-\mathbf{Q})^{-1}(\boldsymbol{1}+\boldsymbol{r})$. Substituting this, (14), and (15) into (13), we obtain $\mathbb{E}[Y]$.

The second-order moment $\mathbb{E}\big[Y^2\big]$ can also be computed via a first-step analysis. This yields

$$\mathbb{E}\big[Y^2|Z^{(1)} = (\text{S},b,\boldsymbol{\ell})\big] = 1, \quad b \in [0:E], \boldsymbol{\ell} \in \mathcal{L}, \qquad (18)$$

$$\mathbb{E}\big[Y^2|Z^{(1)} = (\text{F},b,\boldsymbol{\ell})\big]$$
$$= 1 + 2\sum_{z \in \{\text{F,S}\} \times [0:E] \times \mathcal{L}} \mathbb{E}\big[Y|Z^{(1)} = z\big]\mathbb{P}[(\text{F},b,\boldsymbol{\ell}) \to z]$$
$$+ \sum_{z \in \{\text{F,S}\} \times [0:E] \times \mathcal{L}} \mathbb{E}\big[Y^2|Z^{(1)} = z\big]\mathbb{P}[(\text{F},b,\boldsymbol{\ell}) \to z] \quad (19)$$
$$= -1 + 2\mathbb{E}\big[Y|Z^{(1)} = (\text{F}_b,\boldsymbol{\ell})\big] + r(b,\boldsymbol{\ell})$$
$$+ \sum_{b'' \in [0:E], \boldsymbol{\ell}'' \in \mathcal{L}} \mathbb{E}\big[Y^2|Z^{(1)} = (\text{F},b'',\boldsymbol{\ell}'')\big]$$
$$\cdot q((b,\boldsymbol{\ell}) \to (b'',\boldsymbol{\ell}'')). \qquad (20)$$

Let $\boldsymbol{e}_2$ be a vector that contains $\mathbb{E}\big[Y^2|Z^{(1)} = (\text{F},b,\boldsymbol{\ell})\big]$ for all values of $(b,\boldsymbol{\ell})$. We can express (20) compactly as $(\mathbf{I}-\mathbf{Q})\boldsymbol{e}_2 = -\boldsymbol{1} + 2\boldsymbol{e} + \boldsymbol{r}$. It follows that $\boldsymbol{e}_2 = (\mathbf{I}-\mathbf{Q})^{-1}(-\boldsymbol{1} + 2\boldsymbol{e} + \boldsymbol{r})$. Using this, (14), and (19), we compute $\mathbb{E}\big[Y^2\big]$ via an expansion analogous to (13). Finally, we obtain the average AoI $\bar{\Delta}$ by
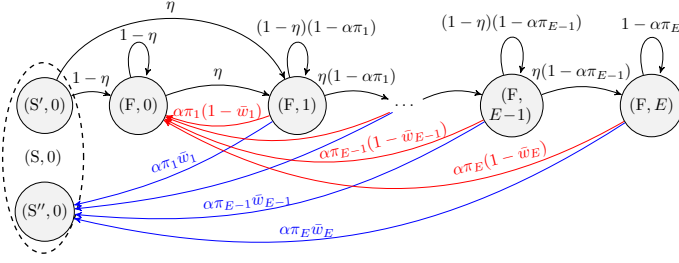
Fig. 3: Markov chain M_2 to track the AoI refresh of a device.

inserting the computed moments of Y into (12).

The above exact computation becomes infeasible when U and E are large. Specifically, computing the transition probabilities between all $2(E+1)\binom{U+E-1}{E}$ states of the chain Z is prohibitive for large U and E. This motivates us to propose an approximate analysis in the next section.

V. APPROXIMATE AoI ANALYSIS

To simplify the analysis, we ignore the time dependency of the battery profile of the devices whose performance is not tracked. Specifically, we assume the following.

Simplification 1: given a device of interest, the battery profile $\boldsymbol{L}$ of the remaining $U-1$ devices is *independent* across slots.

This simplification allows us to analyze the behavior of the system, and, as we shall see, results in tight approximations on the average AoI and AVP for all scenarios explored. Under this simplification, the successful delivery probability of a device that transmits with b energy units is the average of $w_{b,\boldsymbol{L}}$ over $\boldsymbol{L}$, i.e., $\bar{w}_b$ in (1). This allows us to derive the distribution of the inter-refresh time Y in closed form.

1) Distribution of the Inter-Refresh Time Y: To track the behavior of the device of interest, we consider the Markov chain M_2 in Fig. 3, which is obtained from M_1 in Fig. 2 as follows. We split the battery state 0 into two states: AoI refresh $(S,0)$ and no AoI refresh $(F,0)$. The state $b \in [E]$ in M_1 is called (F,b) in M_2. The device visits this state if its AoI value is not refreshed and its battery level is b. After some manipulations, we obtain the transition probabilities between these states under Simplification 1 as depicted in Fig. 3. We can also interpret the chain M_2 as obtained by grouping the states $\{(x,b,\boldsymbol{\ell}) \colon \boldsymbol{\ell} \in \mathcal{L}\}$ of $Z^{(s)}$ into a single state (x,b), and computing the transition probabilities as $\mathbb{P}[(x',b') \to (x,b)] = \mathbb{E}\left[\sum_{\boldsymbol{\ell} \in \mathcal{L}} \mathbb{P}\left[(x',b',\boldsymbol{L}') \to (x,b,\boldsymbol{\ell})\right]\right]$ where the expectation is over the steady state distribution of $\boldsymbol{L}'$. Next, we further split state $(S,0)$ into two states: $(S,0')$ (with only outgoing transitions from $(S,0)$) and $(S'',0)$ (with only incoming transitions to $(S,0)$). The chain M_2 is a *terminating Markov chain* with one absorbing state $(S'',0)$ and $E+1$ transient (i.e., non-absorbing) states $\{(S',0),(F,0),(F,1),\ldots,(F,E)\}$. Observe that the inter-refresh time Y is the absorption time into $(S'',0)$ when starting from $(S',0)$. The distribution of the time until absorption of a terminating Markov chain is called the *discrete phase-type distribution* and has been analyzed in [14, Sec. 2.2]. Leaning on this result, we characterize the distribution of Y in the next lemma, whose proof is omitted due to the space limitations.

Lemma 1 (Distribution of the inter-refresh time): Under Assumption 1, it holds that

$$\mathbb{P}[Y = y] = [\boldsymbol{\mathsf{T}}^{y-1}\boldsymbol{t}_0]_1, \quad y = 1,2,\ldots, \tag{21}$$

$$\mathbb{P}[Y \geq y] = [\boldsymbol{\mathsf{T}}^{y-1}\boldsymbol{1}_{E+1}]_1, \quad y = 1,2,\ldots, \tag{22}$$

where $\boldsymbol{t}_0 = [0 \ \ \alpha\pi_1\bar{w}_1 \ \ \ldots \ \ \alpha\pi_E\bar{w}_E]^{\mathsf{T}}$ and $\boldsymbol{\mathsf{T}}$ is given in (23). Furthermore,

$$\mathbb{E}[Y] = [(\boldsymbol{\mathsf{I}}_{E+1} - \boldsymbol{\mathsf{T}})^{-1}\boldsymbol{1}_{E+1}]_1, \tag{24}$$

$$\mathbb{E}\left[Y^2\right] = 2[(\boldsymbol{\mathsf{I}}_{E+1} - \boldsymbol{\mathsf{T}})^{-2}\boldsymbol{1}_{E+1}]_1 - \mathbb{E}[Y]. \tag{25}$$

2) Approximate Average AoI: By inserting the moments of Y given in (24) and (25) into (12), we obtain the average AoI under Simplification 1 as

$$\bar{\Delta} = \frac{1}{2} + \frac{[(\boldsymbol{\mathsf{I}}_{E+1} - \boldsymbol{\mathsf{T}})^{-2}\boldsymbol{1}_{E+1}]_1}{[(\boldsymbol{\mathsf{I}}_{E+1} - \boldsymbol{\mathsf{T}})^{-1}\boldsymbol{1}_{E+1}]_1}. \tag{26}$$

3) Approximate AVP: Without loss of generality, we start tracking the process (i.e., we set $t=0$) right after the first AoI refresh, which is indexed as the 0th refresh. Let t_i be the time instant of the ith AoI refresh and $y_i = t_i - t_{i-1}$ the duration of the ith inter-refresh period. Using [1, Eq. (15)], we compute the AVP under Simplification 1 as

$$\zeta(\theta) = \lim_{T \to \infty} \frac{1}{T}\int_0^T \mathbb{1}\{\Delta(t) > \theta\}\mathrm{d}t \tag{27}$$

$$= \lim_{m \to \infty} \frac{1}{\sum_{i=1}^m y_i}\sum_{i=1}^m \int_{t_{i-1}}^{t_i} \mathbb{1}\{\Delta(t) > \theta\}\mathrm{d}t \tag{28}$$

$$= \lim_{m \to \infty} \frac{1}{\sum_{i=1}^m y_i}\sum_{i=1}^m (y_i - \theta + 1)^+ \tag{29}$$

$$= \lim_{m \to \infty} \frac{1}{\frac{1}{m}\sum_{i=1}^m y_i}\sum_{y=0}^{\infty} \frac{|\{i \in [m] \colon y_i = y\}|}{m}(y-\theta+1)^+ \tag{30}$$

$$= \frac{1}{\mathbb{E}[Y]}\sum_{y=0}^{\infty}\mathbb{P}[Y = y]\,(y-\theta+1)^+ \tag{30}$$

$$= \frac{1}{\mathbb{E}[Y]}\left(\sum_{y=\theta}^{\infty}y\mathbb{P}[Y = y] - (\theta-1)\sum_{y=\theta}^{\infty}\mathbb{P}[Y = y]\right) \tag{31}$$

$$= 1 - \frac{1}{\mathbb{E}[Y]}\left(\sum_{y=1}^{\theta-1}y\mathbb{P}[Y = y] - (\theta-1)\mathbb{P}[Y \geq \theta]\right) \tag{32}$$

$$= 1 - \frac{\sum_{y=1}^{\theta-1}y[\boldsymbol{\mathsf{T}}^{y-1}\boldsymbol{t}_0]_1 - (\theta - 1)[\boldsymbol{\mathsf{T}}^{\theta-1}\boldsymbol{1}_{E+1}]_1}{[(\boldsymbol{\mathsf{I}}_{E+1} - \boldsymbol{\mathsf{T}})^{-1}\boldsymbol{1}_{E+1}]_1}, \tag{33}$$

where (29) holds because within the ith inter-refresh period, the AoI exceeds θ in the last $(y_i - \theta + 1)^+$ slots (see Fig. 1); (30) holds because $\frac{1}{m}\sum_{i=1}^m y_i \to \mathbb{E}[Y]$ and $\frac{|\{i \in [m] \colon y_i = y\}|}{m} \to \mathbb{P}[Y = y]$ as $m \to \infty$.

VI. NUMERICAL EXPERIMENT

A. Channel Model and Successful Delivery Probability

We assume that a slot comprises n uses of a real-valued AWGN channel. In a slot, active device i with battery level b_i transmits a signal $\sqrt{\frac{b_i}{n}}\boldsymbol{x}_i \in \mathbb{R}^n$ ($\|\boldsymbol{x}_i\| = 1$) with power b_i/n.

The received signal is $\boldsymbol{y} = \sum_{i=1}^{K} \sqrt{b_i/n}\, \boldsymbol{x}_i + \boldsymbol{z}$, where K is the number of active devices and $\boldsymbol{z} \sim \mathcal{N}(0, \sigma^2)$ is the AWGN. The devices transmit at rate R bits/channel use, i.e., $\boldsymbol{x}_i$ belongs to a codebook containing 2^{nR} codewords. We consider shell codes for which the codewords are uniformly distributed on the unit sphere. We analyze two decoding scenarios.

1) Without Capture: In this scenario, all collided packets are lost. Decoding is attempted only on packets transmitted in singleton slots. This model allows us to revisit the collision channel model commonly used in modern random-access analyses, and further account for single-user decoding errors due to finite-blocklength effects. Consider an active device that transmits with b energy units and assume that the battery profile of the remaining $U - 1$ devices is $\boldsymbol{L}$. The successful delivery probability of the device of interest is

$$w_{b,\boldsymbol{L}} = (1 - \epsilon_b)\prod_{i=0}^{E}(1 - \pi_i)^{L_i}, \qquad (34)$$

where ϵ_b is the error probability of decoding the device of interest in a singleton slot. To compute ϵ_b, we use that the maximum achievable rate is [15, Th. 54]

$$R^* = C(b) - \sqrt{\frac{V(b)}{n}} Q^{-1}(\epsilon_b) + O\!\left(\frac{\ln n}{n}\right) \qquad (35)$$

where $C(b) = \frac{1}{2}\log_2\!\left(1 + \frac{b}{n\sigma^2}\right)$, $Q^{-1}(\cdot)$ is the inverse of the Gaussian Q-function $Q(z) = \frac{1}{2\pi}\int_z^{\infty} e^{-t^2/2}\mathrm{d}t$, and $V(b) = \frac{\frac{b^2}{n^2\sigma^4} + 2\frac{b}{n\sigma^2}}{2(\frac{b}{n\sigma^2}+1)^2}\log_2^2(e)$ is the channel dispersion. For a fixed rate R, we use (35) to approximate ϵ_b as $\epsilon_b \approx Q\!\left(\sqrt{\frac{n}{V(b)}}(C(b) - R)\right)$, where we omitted $O(\frac{\ln n}{n})$, which is negligible for large n.

2) With Capture: In this case, the receiver attempts to decode every packet transmitted in a slot by treating all other colliding packets as noise. Consider an active device with battery level b and let the battery profile of the remaining $U - 1$ devices be $\boldsymbol{L}$. Furthermore, assume that out of the other L_i devices with battery level i, $\bar{L}_i$ devices transmit. Then the interference-to-noise power ratio is $\tilde{P} = \frac{1}{n\sigma^2}\sum_{i=0}^{E} i\bar{L}_i$, and the signal-to-interference-plus-noise ratio is $\bar{P} = \frac{b/(n\sigma^2)}{\tilde{P}+1}$. In this setup, an achievable rate for the device of interest is given as in (35) with $C(b)$ and $V(b)$ replaced by $\frac{1}{2}\log_2(1 + \bar{P})$ and $V'(b, \{\bar{L}_i\}) = \frac{\frac{b^2}{n^2\sigma^4}(1 + 2\tilde{P} + \tilde{P}^2 - \breve{P}) + 2\frac{b}{n\sigma^2}(\tilde{P}+1)^3}{2(\breve{P}+1)^2(b/(n\sigma^2)+\tilde{P}+1)^2}\log_2^2 e$, respectively [16, Th. 2]. Here, $\breve{P} = \frac{1}{n^2\sigma^4}\sum_{i=0}^{E} i^2\bar{L}_i$. Given $\{\bar{L}_i\}_{i=0}^{E}$, the error probability of the device is approximated as

$$\epsilon_{b,\{\bar{L}_i\}} \approx Q\!\left(\sqrt{\frac{n}{V'(b,\{\bar{L}_i\})}}\big(\tfrac{1}{2}\log_2(1+\bar{P}) - R\big)\right). \qquad (36)$$

We further assume that the receiver employs SIC. It first decodes all devices that transmit with E energy units, removes

the decoded packets, then decodes all devices that transmit with $E - 1$ energy units, and so on. We assume that the decoding of a packet of energy j is attempted only if all higher-energy packets have been correctly decoded and removed. In this case, the battery profile of the interfering devices becomes $\hat{\boldsymbol{L}}^{(j)} = (\hat{L}_0^{(j)}, \ldots, \hat{L}_E^{(j)})$, where $\hat{L}_i^{(b)} = \bar{L}_i \mathbb{1}\{i \le b\}$; if $j > b$, then $\hat{L}_i^{(j)}$ takes value 0 if $i > j$, value $\bar{L}_i - 1$ if $i = j$, value $\bar{L}_i + 1$ if $i = b$, and value $\bar{L}_i$ if $i < j, i \le b$. It follows that

$$w_{b,\boldsymbol{L}} = \mathbb{E}_{\{\bar{L}_i\}_{i=1}^{E}}\!\left[\big(1 - \epsilon_{b,\hat{\boldsymbol{L}}^{(b)}}\big)\prod_{j>b}\big(1 - \epsilon_{j,\hat{\boldsymbol{L}}^{(b)}}\big)^{\bar{L}_j}\right], \quad (37)$$

where $\bar{L}_i$ follows the binomial distribution with parameters $(L_i, \alpha\pi_i)$. Note that $\hat{\boldsymbol{L}}^{(b)}$ is a function of $(b, \{\bar{L}_i\}_{i=1}^{E})$.

Hereafter, we consider a slot length n of 100 channel uses and transmission rate R of 0.8 bits/channel use.

B. AoI and Throughput Evaluation

We first verify the accuracy of the exact and approximate AoI analysis by comparing with simulation results obtained from an implementation of the complete protocol operations over 10^7 slots. To enable the computation of the exact average AoI, we consider a small system with $U = 30$ and $E = 2$. We further set $\eta = 0.05$, $\theta = 1000$, and $\sigma^2 = -20$ dB. In Fig. 4, we plot the average AoI (normalized by U) and AVP for the considered setting with capture. We consider $\boldsymbol{\pi} = (1,1)$ and $\boldsymbol{\pi} = (0,1)$. In both cases, the approximate average AoI (26) matches well both the simulation results and exact analytical results. The approximate AVP (33) is also in agreement with the simulation result. This confirms that our approximate analysis provides an accurate prediction of the AoI performance.

Next, we report the approximate average AoI and AVP for a larger system with $U = 1000$, $E = 8$, $\eta = 0.005$, and $\theta = 10000$. We optimize $\boldsymbol{\pi}$ to obtain $\boldsymbol{\pi}_{\bar{\Delta}}^* = \arg\min_{\boldsymbol{\pi}\in[0,1]^E} \bar{\Delta}$, $\boldsymbol{\pi}_\zeta^* = \arg\min_{\boldsymbol{\pi}\in[0,1]^E} \zeta(\theta)$, $\boldsymbol{\pi}_S^* = \arg\max_{\boldsymbol{\pi}\in[0,1]^E} S$. We numerically solve these optimization problems using the Nelder-Mead simplex algorithm [17]. In Fig. 5, we plot the minimized average AoI, minimized AVP, and maximized throughput as a function of $U\alpha$, and compare it with two baseline strategies: i) $\boldsymbol{\pi} = (\boldsymbol{0}_{E-1}^{\mathsf{T}}, 1)$, i.e., a device transmits only with full battery, and ii) $\boldsymbol{\pi} = \boldsymbol{1}_E^{\mathsf{T}}$, i.e., a device transmits a new update whenever possible.[2] We see that the optimized $\boldsymbol{\pi}$ leads to significant improvement in all three metrics. The strategy $\boldsymbol{\pi} = \boldsymbol{1}_E^{\mathsf{T}}$ is close to optimal when $U\alpha$ is small, especially with capture. However, this strategy becomes highly suboptimal when $U\alpha$ increases, since it causes many collisions. In contrast, the strategy with

---

[2]The strategy with $\boldsymbol{\pi} = \boldsymbol{1}_E^{\mathsf{T}}$ (best-effort uniform policy) was shown to be average-AoI optimal in the case of infinite battery capacity for the single-source scenario with perfect or packet-erasure channel [8], [9].

$$\boldsymbol{\mathsf{T}} = \begin{bmatrix} 1-\eta & \eta & 0 & 0 & \ldots & 0 & 0 \\ \alpha\pi_1(1-\bar{w}_1) & (1-\eta)(1-\alpha\pi_1) & \eta(1-\alpha\pi_1) & 0 & \ldots & 0 & 0 \\ \alpha\pi_2(1-\bar{w}_2) & 0 & (1-\eta)(1-\alpha\pi_2) & \eta(1-\alpha\pi_2) & \ldots & 0 & 0 \\ \vdots & \vdots & \vdots & \ddots & \ddots & \vdots & \vdots \\ \alpha\pi_{E-1}(1-\bar{w}_{E-1}) & 0 & 0 & 0 & \ldots & (1-\eta)(1-\alpha\pi_{E-1}) & \eta(1-\alpha\pi_{E-1}) \\ \alpha\pi_E(1-\bar{w}_E) & 0 & 0 & 0 & \ldots & 0 & 1-\alpha\pi_E \end{bmatrix} \qquad (23)$$
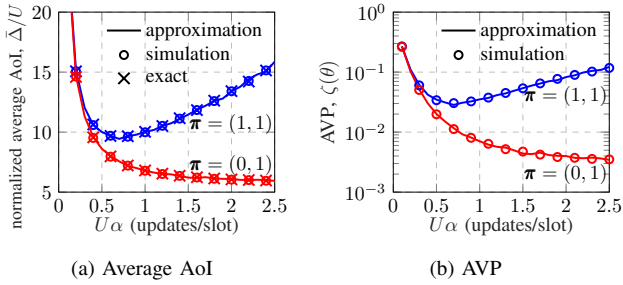
Fig. 4: Average AoI and AVP vs. average total number of new updates in a slot ($U\alpha$). Here, $U = 30$, $\eta = 0.05$, $E = 2$, $n = 100$, $R = 0.8$, $\theta = 1000$, $\sigma^2 = -20$ dB, and the decoder is with capture.

$\boldsymbol{\pi} = (\mathbf{0}_{E-1}^{\mathsf{T}}, 1)$ has a decreasing gap to the optimal performance without capture when $U\alpha$ is large. However, this strategy does not benefit from decoding with capture since the level of interference in non-singleton slots is always high. With capture, the minimized average AoI and maximized throughput are improved by about 10% and 18.7%, respectively, for $U\alpha = 2.5$, compared to decoding without capture.

The optimized $\boldsymbol{\pi}$ can be different for different metrics. While the $\boldsymbol{\pi}$ optimized for the average AoI also performs close to optimal for the AVP and vice versa, the one optimized for throughput leads to suboptimal average AoI and AVP, especially for high $U\alpha$. Without capture, for the optimized $\boldsymbol{\pi}$, devices with higher battery level transmit more often. With capture, the devices transmit with either low or high power, facilitating the decoding of high-energy packets and then of low-energy packets after SIC. For example, for $U\alpha = 2.1$, $\boldsymbol{\pi}_{\bar{\Delta}}^*$ is $(0, 0, 0, 0.68, 1, 1, 1, 1)$ without capture and $(0, 0, 1, 1, 0, 0, 0, 1)$ with capture.

VII. CONCLUSIONS

We studied the impact of energy harvesting on information freshness in slotted ALOHA networks. Leaning on a Markovian analysis, we provided an exact analytical analysis of the average AoI, as well as an approximate analysis that results in easy-to-compute and accurate approximations of both the average AoI and AVP. Our main findings are as follows: i) transmitting a new update whenever possible is beneficial only for low update generation rates, while waiting for sufficient energy before transmitting is preferable for high update generation rates, ii) significant gains with respect to these two baseline strategies can be achieved with an optimized strategy, iii) the AVP-minimizing strategy performs close to optimal in terms of the average AoI and vice versa, while the one optimized for throughput entails a notable loss in terms of the AoI metrics, iv) decoding with capture significantly outperforms decoding without capture, especially for high update generation rates.

REFERENCES

[1] R. D. Yates, Y. Sun, D. R. Brown, S. K. Kaul, E. Modiano, and S. Ulukus, "Age of information: An introduction and survey," *IEEE J. Sel. Areas Commun.*, vol. 39, no. 5, pp. 1183–1210, May 2021.

[2] R. D. Yates and S. K. Kaul, "Status updates over unreliable multiaccess channels," in *Proc. IEEE Int. Symp. Inf. Theory (ISIT)*, Aachen, Germany, Jun. 2017, pp. 331–335.
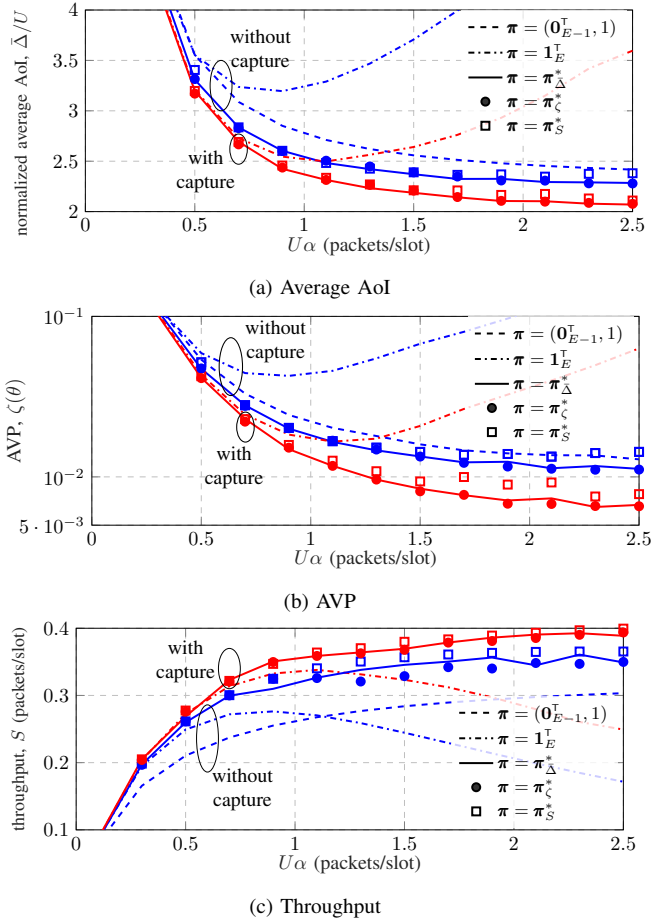
(a) Average AoI

(b) AVP

(c) Throughput

Fig. 5: Approximate average AoI, AVP, and throughput vs. the total number of new updates in a slot ($U\alpha$) for different values of the transmission probabilities $\boldsymbol{\pi}$. With $\boldsymbol{\pi} = (\mathbf{0}_{E-1}^{\mathsf{T}}, 1)$, the performance with capture coincides with that without capture. Here, $U = 1000$, $\eta = 0.005$, $E = 8$, $n = 100$, $R = 0.8$, $\theta = 10000$, and $\sigma^2 = -20$ dB.

[3] A. Munari, "On the value of retransmissions for age of information in random access networks without feedback," in *Proc. IEEE Glob. Commun. Conf. (GLOBECOM)*, Rio de Janeiro, Brazil, Dec. 2022, pp. 4964–4970.

[4] ——, "Modern random access: An age of information perspective on irregular repetition slotted ALOHA," *IEEE Trans. Commun.*, vol. 69, no. 6, pp. 3572–3585, Jun. 2021.

[5] K.-H. Ngo, G. Durisi, and A. Graell i Amat, "Age of information in prioritized random access," in *Proc. Asilomar Conf. Signals, Systems and Computers*, Pacific Grove, CA, USA, Oct. 2021, pp. 1502–1506.

[6] A. Munari, F. Lazaro, G. Durisi, and G. Liva, "The dynamic behavior of frameless ALOHA: Stability, throughput, and age of information," *IEEE Trans. Commun.*, 2023.

[7] P. Kamalinejad, C. Mahapatra, Z. Sheng, S. Mirabbasi, V. C. Leung, and Y. L. Guan, "Wireless energy harvesting for the Internet of Things," *IEEE Commun. Mag*, vol. 53, no. 6, pp. 102–108, Jun. 2015.

[8] X. Wu, J. Yang, and J. Wu, "Optimal status update for age of information minimization with an energy harvesting source," *IEEE Trans. Green Commun. Netw.*, vol. 2, no. 1, pp. 193–204, Mar. 2018.

[9] S. Feng and J. Yang, "Age of information minimization for an energy harvesting source with updating erasures: Without and with feedback," *IEEE Trans. Commun.*, vol. 69, no. 8, pp. 5091–5105, Aug. 2021.

[10] A. M. Ibrahim, O. Ercetin, and T. ElBatt, "Stability analysis of slotted Aloha with opportunistic RF energy harvesting," *IEEE J. Sel. Areas Commun.*, vol. 34, no. 5, pp. 1477–1490, May 2016.

[11] H.-H. Choi, W. Shin, M. Levorato, and H. V. Poor, "Harvest-or-access: Slotted ALOHA for wireless powered communication networks," *IEEE Trans. Veh. Technol.*, vol. 68, no. 11, pp. 11 394–11 398, Nov. 2019.

[12] U. Demirhan and T. M. Duman, "Irregular repetition slotted ALOHA with energy harvesting nodes," *IEEE Trans. Wireless Commun.*, vol. 18, no. 9, pp. 4505–4517, Sep. 2019.

[13] H. M. Taylor and S. Karlin, *An Introduction To Stochastic Modeling*, 3rd ed. London, UK: Academic Press, 1998.

[14] M. F. Neuts, *Matrix-Geometric Solutions in Stochastic Models: An Algorithmic Approach*. Baltimore, Maryland, USA: The Johns Hopkins University Press, 1981.

[15] Y. Polyanskiy, H. V. Poor, and S. Verdu, "Channel coding rate in the finite blocklength regime," *IEEE Trans. Inf. Theory*, vol. 56, no. 5, pp. 2307–2359, May 2010.

[16] J. Scarlett, V. Y. F. Tan, and G. Durisi, "The dispersion of nearest-neighbor decoding for additive non-Gaussian channels," *IEEE Trans. Inf. Theory*, vol. 63, no. 1, pp. 81–92, Jan. 2017.

[17] J. A. Nelder and R. Mead, "A simplex method for function minimization," *The computer journal*, vol. 7, no. 4, pp. 308–313, Jan. 1965.